Vietnam Journal of Catalysis and Adsorption
Tạp chí xúc tác và hấp phụ Việt Nam

http://chemeng.hust.edu.vn/jca/

Modifying platinum microelectrodes with electrochemically reduced graphene oxide for application in electrochemical ascorbic acid sensor

Tran Thi Luyen[1*], Tran Vinh Hoang[1]

[1] *School of Chemical Engineering, Hanoi University of Science and Technology, Hanoi, VIETNAM*
**Email: luyen.tranthi@hust.edu.vn*

-Hội thảo quốc tế về Khoa học và Kỹ thuật Phân tách tiên tiến lần thứ hai (CASSE 2022)-

ARTICLE INFO

Received: 02/12/2022
Accepted: 20/5/2023
Published: 30/6/2023

Keywords:

Electrochemically reduced graphene oxide, Electrochemical sensor, Ascorbic acid, Platinum microelectrode, Linear sweep voltammetry

ABSTRACT

Graphene oxide drop-casted on a platinum microelectrode was successfully changed to reduced graphene oxide by using a cyclic voltammetry method. The presence of an electrochemically reduced graphene oxide layer on the platinum electrode was proved by using scanning electron microscopy images, Raman and Fourier-transform infrared spectroscopy spectra. Cyclic voltammetry and linear sweep voltammetry results indicated that the platinum microelectrode modified with electrochemically reduced graphene oxide can be used as an electrochemical sensor for detection of ascorbic acid in aqueous solutions. In a cyclic voltammetry scan and a linear sweep voltammetry curve corresponding to the presence of ascorbic acid, a peak related to the direct oxidation of ascorbic acid appears. The electrochemical sensor based on the electrochemically reduced graphene oxide material works effectively with a detection limit of 0.04 mM, a detection linear range from 0.04 mM to 1.0 mM, a good repeatability, and especially, a rapid detection time thanks to a direct ascorbic acid detection based on the oxidation of ascorbic acid.

Introduction

Graphene oxide (GO) and reduced graphene oxide (rGO) are interesting carbon nanomaterials which have special properties including large surface area, high thermal conductivity, good biocompatibility, chemical stability, mechanical strength and cost effectiveness [1]. Thanks to excellent electrochemical and electrocatalytic characteristics, GO and rGO can be used in various applications such as electrochemical sensors/ biosensors, supercapacitors, batteries and fuel cells [2-5].

For the field of electrochemical sensors, GO and rGO play an important role in improving analytical performance [6]. rGO has a higher electrical conductivity than GO. As a result, rGO is often selected in the fabrication of electrochemical sensors [7, 8]. There are different methods used to synthesize rGO from GO, including chemical and electrochemical processes. In particular, electrochemical methods show many advantages such as good control and high reproducibility [9, 10].

In this study, platinum (Pt) microelectrodes are modified with electrochemically reduced graphene

https://doi.org/10.51316/jca.2023.034

oxide (ERGO) using a simple and effective protocol. These Pt/ERGO microelectrodes are able to be used as electrochemical sensors for direct and rapid detection of ascorbic acid (AA) in aqueous solutions using linear sweep voltammetry (LSV) measurements. The detection linear range and detection limit of the obtained sensor for AA are also investigated.

Experimental

Chemicals and instrumentation

GO was fabricated using Hummer's method as in our previous work [11]. Phosphate buffer solution (PBS) and L-ascorbic acid ($C_6H_8O_6$, ≥99 wt%) were purchased from Sigma Aldrich. Potassium dichromate ($K_2Cr_2O_7$, ≥99 wt%) and sulfuric acid (H_2SO_4, ≥98 wt%) were of analytical grade.

A DY2200 Series Mini Potentiostat/Galvanostat (Digi-Ivy, USA) and a three-electrode system consisting of a Pt microelectrode as a working electrode (WE), a Pt plate as a counter electrode (CE), and an Ag/AgCl electrode in 3 M KCl solution as a reference electrode (RE) were used to perform electrochemical experiments. The Pt microelectrode's configuration and fabrication were described in a previous work [12].

Scanning electron microscopy (SEM) images were recorded using a Nova NanoSEM 450 microscope (FEI Company, Netherlands). Raman and Fourier transform infrared spectroscopy (FT-IR) spectra were investigated using a LabRAM HR 800 Raman (Horiba Jobin Yvon, France) and an IRAffinity-1S FTIR spectrometer (Shimadzu, Japan), respectively.

Electrosynthesis of ERGO on Pt microelectrodes

A saturated $K_2Cr_2O_7/H_2SO_4$ solution was used to clean the Pt microelectrode. After that, 1.0 µL of a 0.5 mg mL^{-1} GO suspension was drop-casted on the Pt microelectrode. ERGO was directly synthesized on the Pt microelectrode using a cyclic voltammetry (CV) experiment performed in a PBS with pH 7.4 at a voltage range from 0.1 V to −1.2 V for 3 cycles and a scan rate of 5 mV s^{-1}.

Detection of AA using Pt/ERGO microelectrodes

The obtained Pt/ERGO microelectrode was used as an electrochemical sensor to detect AA in aqueous solutions. CV and LSV measurements were recorded at a voltage range from −0.2 V to 1.4 V and a scan rate of 50 mV s^{-1}. LSV scans of Pt/ERGO electrodes were conducted in AA solutions with different AA concentrations ranging from 0.04 mM to 1.0 mM to study the sensitivity of the fabricated electrochemical sensor.

Results and discussion

Material characteristics

Figure 1 depicts the SEM images of the fabricated GO and ERGO. There is no change in the surface morphology when GO is electrochemically reduced to form ERGO on the Pt microelectrode.

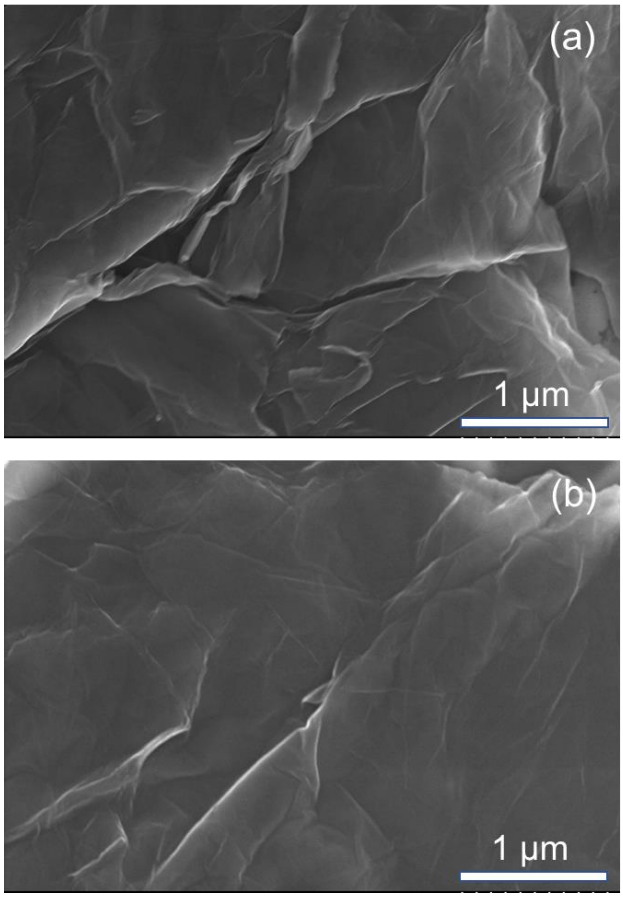

Figure 1: SEM images of (a) GO and (b) ERGO

Figure 2 shows Raman spectra of the obtained GO and ERGO materials. In both Raman spectra, there are two peaks at 1337 cm^{-1} and 1590 cm^{-1} relating to D and G bands of GO and ERGO. The value of I_D/I_G = 1.79 corresponding to the Raman spectrum of ERGO, is higher than the value of I_D/I_G = 0.97 corresponding to the Raman spectrum of GO.

The FT-IR spectra of the synthesized GO and ERGO materials are exhibited in Figure 3. It can be seen in Figure 3 (curve a), the FT-IR spectrum of GO, the

https://doi.org/10.51316/jca.2023.034

bands at 3208 and 1714 cm^{-1} associated with the stretching vibrations of O–H and C=O (in COOH), respectively, appear [13]. The bands at 1047, 1217 and 1405 cm^{-1} assigned to the C–O, C–O–C and O–H (C–OH) stretching vibrations, in the order, are observed [13-15]. Moreover, there is the band at 1598 cm^{-1} related to the C=C stretching mode [14]. In contrast, in Figure 3 (curve b) showing the FT-IR spectrum of ERGO, the bands at 3208, 1714, 1047, 1217 and 1405 cm^{-1} are not observed. Figure 3 (curve b) describes the bands at 1008, 1136 and 1570 cm^{-1}, associated with the C–O and C=C stretching vibrations [15, 16].

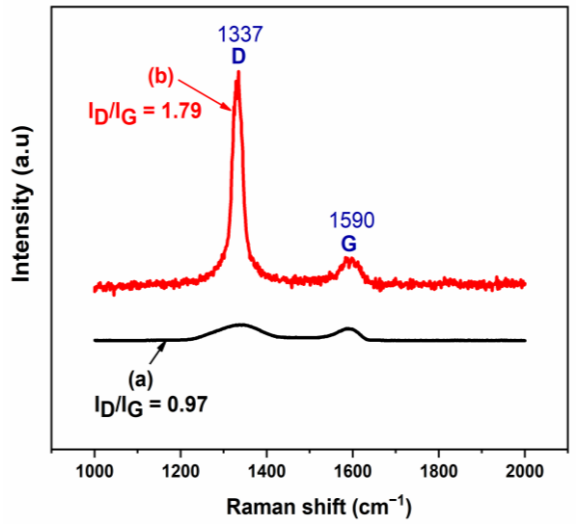

Figure 2: Raman spectra of (a) GO and (b) ERGO.

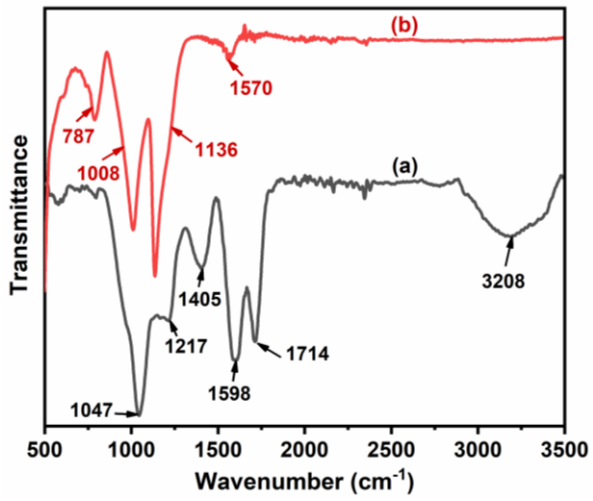

Figure 3: FT-IR spectra of (a) GO and (b) ERGO

The Raman and FT-IR results illustrated in Figure2 and Figure 3 indicate that ERGO is successfully synthesized on the Pt microelectrode by electrochemically reducing GO [10].

Using the Pt/ERGO microelectrode as an electrochemical sensor for AA detection

Figure 4 describes CV scans of Pt (curve a), Pt/GO (curve b), and Pt/ERGO (curve c) microelectrodes recorded in a 5.0 mM AA solution at a scan rate of 50 mV s^{-1}. It is clearly seen that in both CV results corresponding to Pt, Pt/GO, and Pt/ERGO microelectrodes, anodic peaks at 0.82 V, 0.82 V, and 1.08 V, respectively, which are associated with the oxidation of AA (illustrated in Figure 5), can be observed. The anodic peak currents are 34.68 µA, 32.66 µA and 64.64 µA, in the order. The anodic peak current of Pt/ERGO microelectrode is higher than that of Pt and Pt/GO microelectrodes.

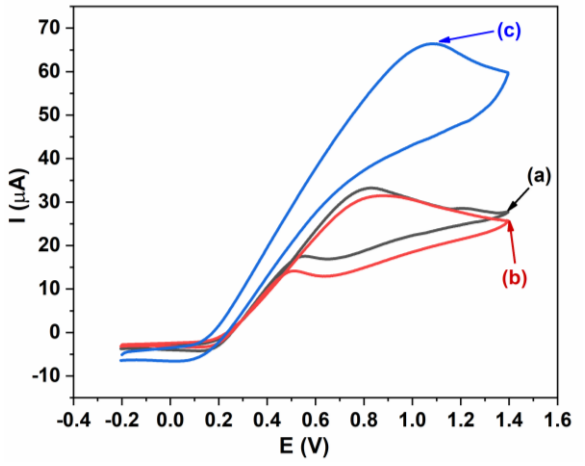

Figure 4: CV results of (a) Pt, (b) Pt/GO, and (c) Pt/ERGO microelectrodes measured in a 5.0 mM AA solution at a scan rate of 50 mV s^{-1}

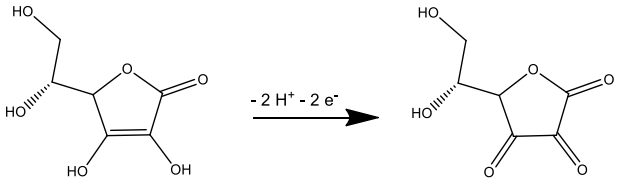

Figure 5: The oxidation of AA

These results prove that the reduction of GO to form ERGO has an important significance in improving the conductivity of the material immobilized on the WE's surface, as a result, the electrochemical signal of the sensor is enhanced.

It is clearly observed in Figure 6, the LSV result of the Pt/ERGO microelectrode measured in distilled water at a scan rate of 50 mV s^{-1} (curve a) has no peak. In contrast, in its LSV result conducted in a 1.0 mM AA solution at the same scan rate (curve b), an obvious peak, which is related to the oxidation of AA (illustrated in Figure 5), appears at 0.80 V with a peak current of 8.38 µA.

LSV results of Pt/ERGO microelectrodes measured in a 2.5 mM AA solution at different scan rates of 5, 10, 20,

https://doi.org/10.51316/jca.2023.034

and 50 mV s^{-1} are exhibited in Figure 7A. The relationship between the peak current (I_{peak}) and the square root of the scan rate ($v^{1/2}$) was investigated based on Figure 7A, and is shown in Figure 7B: I_{pa} (µA) = 2.2991 × $v^{1/2}$ ((mV s^{-1})$^{1/2}$) + 3.9876 (R^2 = 0.9983). This linear relationship indicates that the electro-oxidation of AA is a diffusion-controlled process [17].

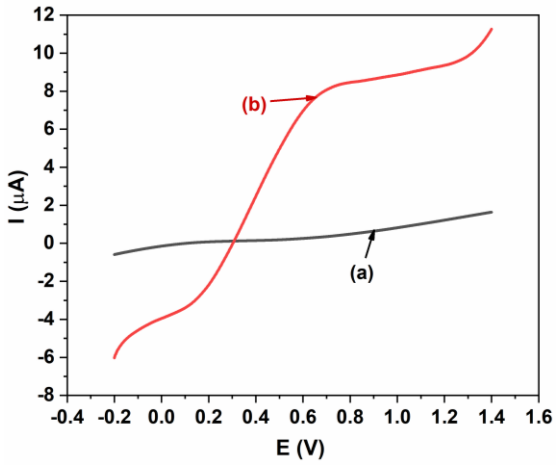

Figure 6: LSV results of Pt/ERGO microelectrodes measured in (a) distilled water and (b) a 1.0 mM AA solution at a scan rate of 50 mV s^{-1}

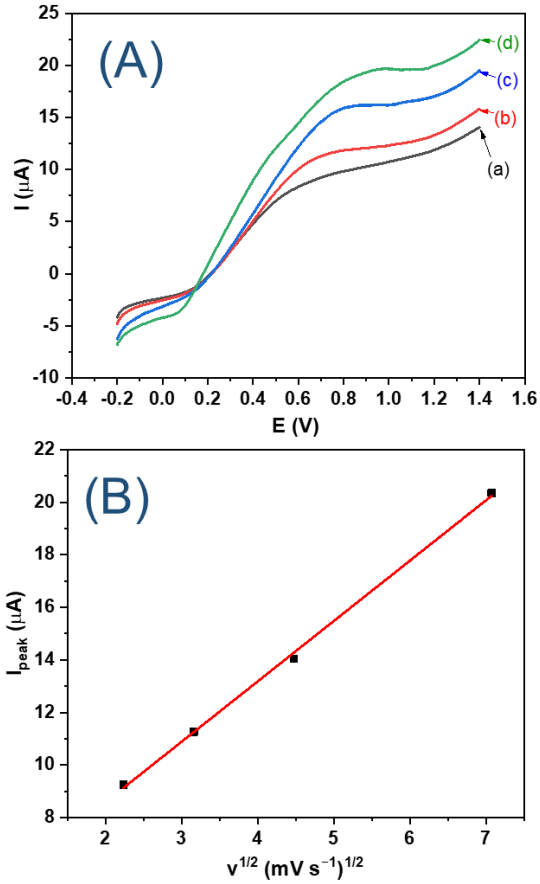

Figure 7: (A) LSV results of Pt/ERGO microelectrodes measured in a 2.5 mM AA solution at different scan rates of (a) 5, (b) 10, (c) 20, and (d) 50 mV s^{-1}; and (B) the linear relationship between I_{peak} (µA) and $v^{1/2}$ ((mV s^{-1})$^{1/2}$)

LSV scans of the Pt/ERGO electrodes conducted in AA solutions with different AA concentrations changing from 0.04 mM to 1.0 mM shown in Figure 8A indicate that the peak current related to the oxidation of AA increases when the concentration of AA increases.

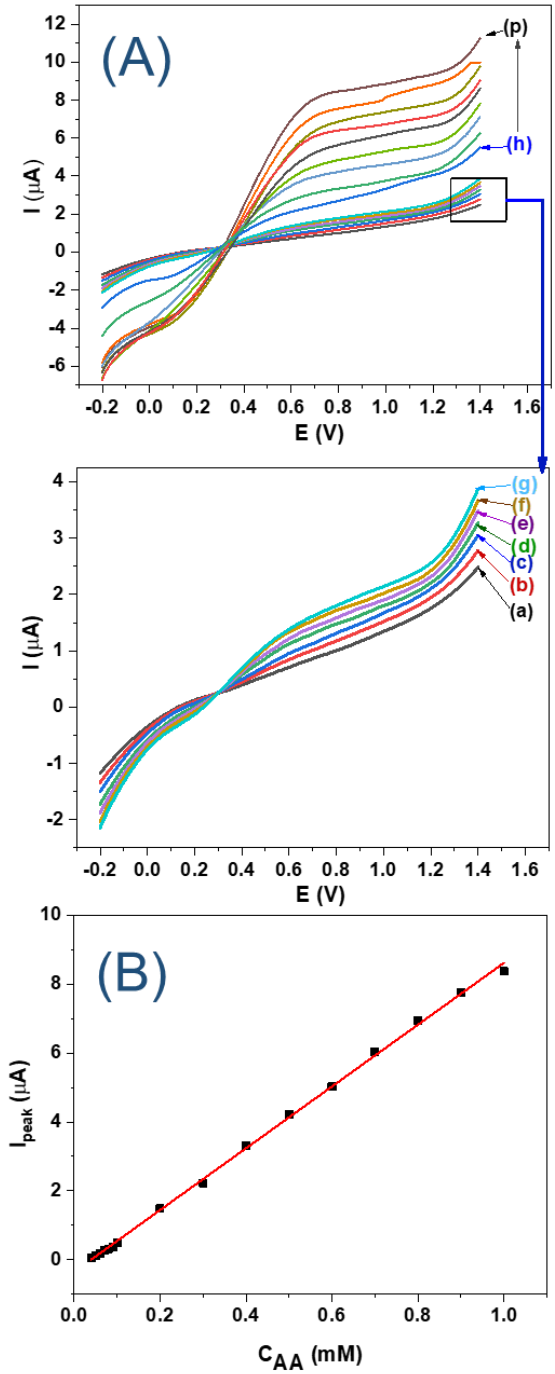

Figure 8: (A) LSV scans of Pt/ERGO electrodes performed at a scan rate of 50 mV s^{-1} in AA solutions with different concentrations of AA: (a) 0.04 mM, (b) 0.05 mM, (c) 0.06 mM, (d) 0.07 mM, (e) 0.08 mM, (f)

https://doi.org/10.51316/jca.2023.034

0.09 mM, (g) 0.1 mM, (h) 0.2 mM, (i) 0.3 mM, (j) 0.4 mM, (k) 0.5 mM, (l) 0.6 mM, (m) 0.7 mM, (n) 0.8 mM, (o) 0.9 mM, (p) 1.0 mM; and (B) the linear relationship between I_{peak} (μA) and C_{AA} (mM)

The linear relationship between the peak current (I_{peak}) and the concentration of AA (C_{AA}) is studied and described in Figure 8B. Figure 8B depicts that the linear equation is I_{peak} (μA) = 8.9578 C_{AA} (mM) – 0.3456 with the correlation coefficient of R^2 = 0.9990. The detection limit of the fabricated sensor is 0.04 mM, using the LOD calculation [18]. Besides, the repeatability of the fabricated sensor for AA detection was investigated, and the obtained results are exhibited in Figure 9. As can be seen in Figure 9, three LSV scans corresponding to three Pt/ERGO electrodes measured in a 2.5 mM AA solution (curve a, curve b, and curve c, respectively) indicate that the electrochemical sensor based on Pt/ERGO electrode has a good repeatability with an error of 2.6%.

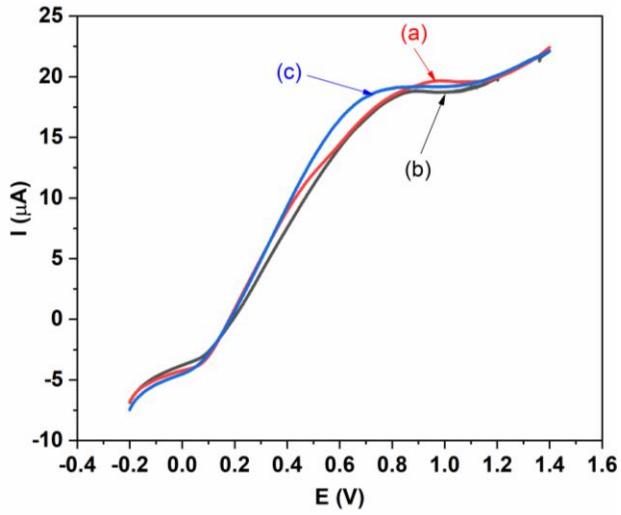

Figure 9: LSV scans of three fabricated Pt/ERGO electrodes performed at a scan rate of 50 mV s^{-1} in a 2.5 mM AA solution

The CV and LSV results described in Figure 4, Figure 6, Figure 8, and Figure 9 prove that the fabricated Pt/ERGO microelectrode can be used as the electrochemical sensor for direct detection of AA with a quite high sensitivity, a rapid detection time, and a good repeatability.

Conclusion

In our work, a Pt microelectrode was modified with ERGO. A simple and effective CV protocol was used to synthesize ERGO from GO drop-casted on the Pt microelectrode. SEM images, Raman and FT-IR spectra have demonstrated the formation of the ERGO layer on the Pt microelectrode. In CV and LSV curves corresponding to the presence of AA in an aqueous solution, there is a significant peak associated with the direct oxidation of AA. CV scans of Pt, Pt/GO and Pt/ERGO electrodes recorded in a AA solution have also indicated that ERGO with an improved electrical conductivity plays an important role in enhancing the output signal of the electrochemical sensor. The fabricated electrochemical sensor can detect AA in aqueous solutions using LSV method with the detection linear range from 0.04 mM to 1.0 mM and the detection limit of 0.04 mM. Our study initially proved that the Pt microelectrode modified with ERGO is able to be used as an effective electrochemical sensor for direct and rapid detection of AA in aqueous solutions with a quite high sensitivity and a good repeatability.

Acknowledgments

This research was funded by Vietnam Ministry of Education and Training (MOET) under grant number CT 2022.04.BKA.04.

References

1. X. Wang, R. Niessner, D. Tang, D. Knopp, Anal. Chim. Acta 912 (2016) 10-23. https://10.1016/j.aca.2016.01.048
2. S. Chen, Y. F. Cheng, G. Voordouw, Sens. Actuators, B 262 (2018) 860-868. https://10.1016/j.snb.2018.02.093
3. T. L. Tran, T. T. Nguyen, T. T. H. Tran, V. T. Chu, Q. T. Tran, A. T. Mai, Phys. E 93 (2017) 83-86. https://10.1016/j.physe.2017.05.019
4. L. F. Aval, M. Ghoranneviss, G. B. Pour, Heliyon 4 (2018) e00862. https://10.1016/j.heliyon.2018.e0086200862
5. W. Li, R. Fang, Y. Xia, W. Zhang, X. Wang, X. Xia, J. Tu, Batteries. Supercaps 2 (2019) 9-36. https://10.1002/batt.201800067
6. J. Sethi, M. V. Bulck, A. Suhail, M. Safarzadeh, A. Perez-Castillo, G. Pan, Microchim. Acta 187 (2020) 288. https://10.1007/s00604-020-04267-x
7. B. Patella, M. Buscetta, S. Di Vincenzo, M. Ferraro, G. Aiello, C. Sunseri, E. Pace, R. Inguanta, C. Cipollina, Sens. Actuators, B 327 (2021) 128901. https://doi.org/10.1016/j.snb.2020.128901

8. D. T. M. Hue, T. T. Luyen, H. T. L. Giang, T. V. Hoang, Vietnam J. Chem., 60 (2022) 46-52. https://10.1002/vjch.202200064
9. L. T. Tran, H. V. Tran, T. Tran, N. T. Nguyen, D. V. Bui, P. Q. Tran, T. V. Chu, J. Electrochem. Soc. 168 (2021) 057518. https://10.1149/1945-7111/ac001b
10. L. T. Tran, H. V. Tran, H. T. M. Dang, A. V. Nguyen, T. H. Tran, C. D. Huynh, RSC Adv. 11 (2021) 19470-19481. https://10.1039/D1RA01301G
11. H. V. Tran, L. T. Bui, T. T. Dinh, D. H. Le, C. D. Huynh, A. X. Trinh, Mater. Res. Express 4 (2017) 035701. https://10.1088/2053-1591/aa6096
12. N. T. Thuy, P. D. Tam, M. A. Tuan, A.T. Le, L. T. Tam, V. V. Thu, N. V. Hieu, N. D. Chien, Curr. Appl. Phys. 12 (2012) 1553-1560. https://10.1016/j.cap.2012.04.035
13. M. Mitra, K. Chatterjee, K. Kargupta, S. Ganguly, D. Banerjee, Diamond Relat. Mater. 37 (2013) 74-79. https://10.1016/j.diamond.2013.05.003
14. Q. Gong, H. Han, H. Yang, M. Zhang, X. Sun, Y. Liang, Z. Liu, W. Zhang, J. Qiao, J Materiomics. 5 (2019) 313-319. https://10.1016/j.jmat.2019.03.004
15. B. D. Ossonon, D. Bélanger, RSC Adv. 7 (2017) 27224-27234. https://10.1039/C6RA28311J
16. M. Mitra, C. Kulsi, K. Chatterjee, K. Kargupta, S. Ganguly, D. Banerjee, S. Goswami, RSC Adv. 5 (2015) 31039-31048. https://10.1039/c5ra01794g
17. C. Guo, Y. Wang, Y. Zhao, C. Xu, Anal. Methods. 5 (2013) 1644-1647. https://10.1039/C3AY00067B
18. H. V. Tran, B. Piro, S. Reisberg, L. D. Tran, H. T. Duc, M. C. Pham, Biosens. Bioelectron. 49 (2013) 164-169. https://10.1016/j.bios.2013.05.007